ARTICLES
PUBLISHED ONLINE: 20 APRIL 2014 | DOI: 10.1038/NCHEM.1924
nature chemistry

A mitochondrial pathway for biosynthesis of lipid mediators

Yulia Y. Tyurina[1,2]*, Samuel M. Poloyac[3], Vladimir A. Tyurin[1,2], Alexander A. Kapralov[1,2], Jianfei Jiang[1,2], Tamil Selvan Anthonymuthu[1,4], Valentina I. Kapralova[1,2], Anna S. Vikulina[1,2,5], Mi-Yeon Jung[1,2], Michael W. Epperly[6], Dariush Mohammadyani[7], Judith Klein-Seetharaman[8], Travis C. Jackson[4], Patrick M. Kochanek[4], Bruce R. Pitt[2,7], Joel S. Greenberger[6], Yury A. Vladimirov[5], Hülya Bayır[1,4]* and Valerian E. Kagan[1,2]*

The central role of mitochondria in metabolic pathways and in cell-death mechanisms requires sophisticated signalling systems. Essential in this signalling process is an array of lipid mediators derived from polyunsaturated fatty acids. However, the molecular machinery for the production of oxygenated polyunsaturated fatty acids is localized in the cytosol and their biosynthesis has not been identified in mitochondria. Here we report that a range of diversified polyunsaturated molecular species derived from a mitochondria-specific phospholipid, cardiolipin (CL), is oxidized by the intermembrane-space haemoprotein, cytochrome *c*. We show that a number of oxygenated CL species undergo phospholipase A_2-catalysed hydrolysis and thus generate multiple oxygenated fatty acids, including well-known lipid mediators. This represents a new biosynthetic pathway for lipid mediators. We demonstrate that this pathway, which includes the oxidation of polyunsaturated CLs and accumulation of their hydrolysis products (oxygenated linoleic, arachidonic acids and monolysocardiolipins), is activated *in vivo* after acute tissue injury.

Mitochondria of eukaryotic cells contain machinery capable of oxidizing substrates in a coupled enzymatic and electrochemical process that effectively generates energy in the form of ATP. In addition to the powerhouse function, mitochondria are now viewed as the major regulatory platform involved in numerous intra- and extracellular metabolic and physiological pathways (from synthesis of major intracellular biomolecules to assembly of inflammasomes, immune responses, generation of reactive oxygen species, dynamic regulation of their own organization via fission and/or fusion and mitophagy, as well as control and execution of apoptotic and necrotic cell death[1]). Although there is an intuitive necessity for the existence of specific signals for mitochondrial communications, the identification of these signals has not been fully achieved. An array of lipid mediators, with diversified and potent signalling effects on the normal homeostasis and responses to stress and disease, is generated through oxygenation of free polyunsaturated fatty acids (PUFAs). Molecular machinery involved in the production of these bioactive oxygenated compounds has been assigned mostly to the cytosol[2]. Surprisingly, mitochondria have not been identified as a site of lipid-mediator biosynthesis[3].

The rate-limiting step in the production of lipid mediators is the availability of oxidizable PUFAs[4]. Normally esterified into cellular (phospho)lipids, free PUFAs are released by Ca^{2+}-dependent phospholipases A_2 (PLA_2) and act as substrates for oxygenation reactions by several enzymes, including cyclooxygenases (COXs), lipoxygenases (LOXs), cytochrome P450 isoforms and peroxidases[5]. A plethora of lipid regulators, including prostaglandins, prostacyclins, thromboxanes, resolvins, protectins, maresins, leukotrienes, lipoxines, lipoxenes, levuloglandins, among others, with a multitude of physiological effects are formed[6,7]. Notably, the major precursor of lipid mediators, phosphatidylserine (PS)[8], is lacking from mitochondria[9]. The majority of phospholipids that constitute the inner and outer mitochondrial membranes (IMM and OMM, respectively) are manufactured outside the organelle, with the notable exception of mitochondria-specific cardiolipin (CL (1,3-bis(*sn*-3′-phosphatidyl)-*sn*-glycerol)). CL is structurally unique as it contains two phosphatidyl groups linked to a glycerol backbone and four fatty acyl chains. With about 20 different residues, mostly PUFAs, available for esterification, the diversity of CL and its oxygenated species may be very high, and thus make it an exceptionally good source of lipid mediators.

The final rate-limiting step in the production of CL takes place in the IMM to which the newly synthesized CL molecules are sequestered, and thus generates characteristic CL asymmetry[10]. Collapse of CL asymmetry and accumulation of its oxygenated products have been identified as essential early steps of apoptosis that culminate in the release of pro-apoptotic factors[11]. CL oxygenation is catalysed by CL/cytochrome *c* (cyt *c*) complexes that act as a potent CL-specific peroxidase[11] via an enzymatic mechanism similar to that of cyclooxygenase-2 (COX-2)-catalysed oxygenation of arachidonic acid (AA)[12]. Given that reactions driven by cyt *c* yield a highly diversified set of oxidized CL (CL_{ox}) products, which include different stereoisomers with hydroperoxy-, hydroxy-, epoxy- and oxofunctionalities[13,14], we hypothesized that mitochondrial CLs could be a

[1]Center for Free Radical and Antioxidant Health University of Pittsburgh, Pittsburgh, Pennsylvania 15213, USA, [2]Department of Environmental Health, Graduate School of Public Health, University of Pittsburgh, Pittsburgh, Pennsylvania 15213, USA, [3]Department of Pharmaceutical Sciences, School of Pharmacy, University of Pittsburgh, Pittsburgh, Pennsylvania 15213, USA, [4]Departments of Critical Care Medicine, Safar Center for Resuscitation Research, University of Pittsburgh, Pittsburgh, Pennsylvania 15213, USA, [5]Department of Biophysics, MV Lomonosov Moscow State University, Moscow 117192, Russia, [6]Radiation Oncology, School of Medicine, University of Pittsburgh, Pittsburgh, Pennsylvania 15213, USA, [7]Department of Bioengineering, Swanson School of Engineering, University of Pittsburgh, Pittsburgh, Pennsylvania 15213, USA, [8]Division of Metabolic and Vascular Health, University of Warwick, Coventry CV4 7AL, UK. *e-mail: yyt1@pitt.edu; bayihx@ccm.upmc.edu; kagan@pitt.edu

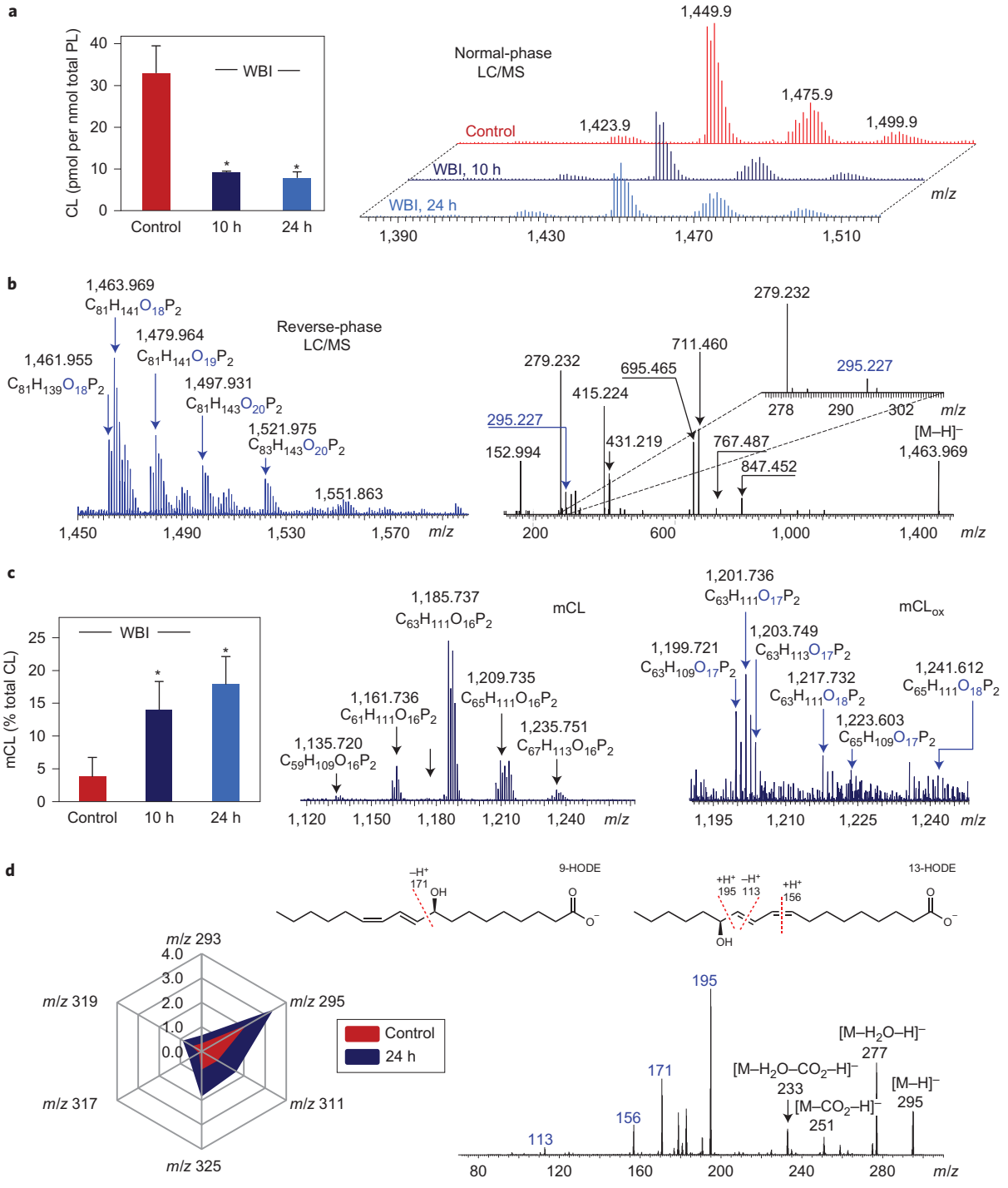

Figure 1 | Exposure of mice to WBI causes CL oxidation and accumulation of its hydrolysis products in the small intestine. a, Quantitation of polyunsaturated CL (left) and MS spectra of CL before and after WBI (10 Gy) (right). Each cluster included 4–5 signals with differing *m/z*. **b**, Typical MS spectrum of CL_{ox} obtained ten hours after WBI (left) and fragmentation pattern (right) of the molecular ion with *m/z* 1,463.969 that contained LA_{ox} (*m/z* 295.227). **c**, Quantitation of total mCL (left), and MS spectra of mCL (middle) and of mCL_{ox} (right). Both mono- and dioxygenated molecular species of mCL_{ox} were detected ten hours after WBI, whereby the mCL_{ox} species were predominant. **d**, Quantitation of $PUFA_{ox}$ accumulated after WBI (left) and the MS/MS spectrum of molecular ion with *m/z* 295 (right). On the radar chart (left) data are presented as picomoles per nanomoles of total phospholipids. Molecular species of $PUFA_{ox}$ were represented by LA_{ox} with *m/z* 293 (13-KODE, 9-KODE), *m/z* 295 (13-HODE, 9-HODE, 9,10-epoxyoctadecenoic acid (9,10-EpOME), 12,13-EpOME, *m/z* 311 (9-HpODE, 8,13-dihydroxyoctadecadienoic acid (DiHODE)), *m/z* 325 (9,14-KHpODE, 9,14-HpKODE, 8,13-KHpODE, 8,13-HpKODE) and AA_{ox} with *m/z* 319 (12-HETE) and *m/z* 317 (15-KETE). Data are means ± s.d., $^*P < 0.05$ versus control, $n = 5$.

source of bioactive lipid mediators. Although lipid mediators, particularly eicosanoids, have been implicated in the regulation of intrinsic and extrinsic apoptotic pathways[15], mitochondria have not been associated with their biosynthesis. Here we report that CL is oxidized by cyt *c* to give highly diversified polyunsaturated molecular species, and thereby represents a new biosynthetic pathway for lipid-mediator production. A rich assortment of CL_{ox} species subsequently undergoes hydrolysis by Ca^{2+}-independent PLA_2 (iPLA$_2\gamma$), and thus generates

multiple oxygenated fatty acids (FA_{ox}), which include well-known lipid mediators as well as oxygenated species of lyso-CLs with yet-to-be determined biological functions.

Results

Selective oxidation and hydrolysis of CL in the mouse small intestine. To ascertain whether mitochondrial CL can be a source of lipid mediators, we performed lipidomic analysis of two different tissues (small intestine and brain) after whole-body irradiation (WBI) and controlled cortical impact (CCI), respectively. In the small intestine (a radiosensitive tissue) of C57BL6 mice exposed to 10 Gy WBI, liquid chromatography/mass spectrometry (LC/MS) analysis revealed: (1) a decrease of oxidizable polyunsaturated CL molecular species (Fig. 1a), (2) generation of CL_{ox} (Fig. 1b) and (3) accumulation of monolysocardiolipins (mCLs) (Fig. 1c) and FA_{ox} (Fig. 1d). CL_{ox} were represented mainly by molecular species that contained one, two or three additional oxygen atoms and their structures were confirmed by MS/MS analysis (Fig. 1b). Although mCLs included mainly non-oxidized molecular species, both mono- and dioxygenated species of mCL (mCL_{ox} and dCL_{ox}, respectively), particularly with mono- and dioxygenated linoleic acid (mLA_{ox} and dLA_{ox}, respectively), were also detected (Supplementary Fig. 1 and Supplementary Table 1), of which the mCL_{ox} derivatives were predominant (Fig. 1c). Quantitatively, the amount of detectable CL_{ox} (0.12 ± 0.05 pmol per nmol total phospholipids) was ~2.5 times lower than the level of mCL (0.30 ± 0.18 pmol per nmol total phospholipids). This indicates that the hydrolysis reactions (possibly catalysed by $iPLA_2\gamma$) were effective in converting CL_{ox} into mCLs. The major FA_{ox} species (mostly mLA_{ox} derivatives) were 9-hydroxyoctadecadienoic acid (9-HODE) and 13-HODE (Fig 1d). In addition, 9-oxo-octadecadienoic acid (9-KODE) and 13-KODE, 9-hydroperoxyoctadecadienoic acid (9-HpODE) and 13-HpODE, 12-hydroxyeicosatetraenoic acid (12-HETE) and 15-HETE, and 15-oxo-eicosatetraenoic acid (15-KETE) were also detectable, albeit in significantly smaller amounts (Supplementary Fig. 2 and Supplementary Table 2).

To ascertain whether $iPLA_2\gamma$ might be accountable for the hydrolysis of CL_{ox} that leads to the generation of mCLs, we utilized (*R*)-BEL (6*E*-(bromoethylene)tetrahydro-3*R*-(1-naphthalenyl)-2H-pyran-2-one), an inhibitor of $iPLA_2\gamma$), *in vivo*[16]. We confirmed that (R)-BEL did not inhibit peroxidase activity of cyt *c*/CL complexes (Supplementary Table 3). (R)-BEL blocked the irradiation-induced accumulation of mCL by $94.9 \pm 0.7\%$. Irradiation-induced accumulation of two major lysophosphatidylcholines (LPCs) (16:0-LPC and 18:0-LPC) was not affected significantly by (*R*)-BEL (data not shown). The amount of detectable CL_{ox} in the small intestine of mice pretreated with (*R*)-BEL and exposed to WBI was estimated as 0.29 ± 0.15 pmol per nmol total phospholipids, a ~2.5-fold increase versus its content in the absence of the inhibitor. Thus, $iPLA_2\gamma$ is mainly responsible for the hydrolysis of CL_{ox} and the production of mCL. Simultaneously, the total amount of released FA_{ox} was inhibited by $67.3 \pm 7.2\%$. In particular, 12-HETE and 15-HETE concentrations in irradiated intestinal samples from (*R*)-BEL-treated animals were $45.7 \pm 16.0\%$ and $76.3 \pm 28.0\%$, respectively, of untreated irradiated intestinal samples. As expected, the decrease of oxidizable CL species was not affected significantly by (*R*)-BEL (data not shown). Overall, these data emphasize the major role of $iPLA_2\gamma$ in the generation of mCLs and also reflect the probable involvement of other pathways (independent of $iPLA_2\gamma$) in the formation of FA_{ox}.

We next compared the effects of a cocktail of several reportedly effective inhibitors of COX-, LOX- and cytochrome P450-driven conventional biosynthetic mechanisms for lipid mediator species versus their generation via CL-dependent pathways. Specifically, we tested the effects of the inhibitors of (1) COX-1 and -2 (piroxicam (4-hydroxy-2-methyl-*N*-2-pyridinyl-2*H*-1,2-benzothiazine-3-carboxamide-1,1-dioxide)), (2) LOX (licofelone (6-(4-chlorophenyl)-2,3-dihydro-2,2-dimethyl-7-phenyl-1H-pyrrolizine-5 acetic acid)) and (3) cytochrome P450 epoxygenase/12-HETE activity (CYP2C (MS-PPOH (*N*-(methylsulfonyl)-2-(2-propynyloxy)-benzene hexanamide))[17–20] on the formation of FA_{ox} in the small intestine of irradiated mice. As all three enzymes (COX, P450 and 5-LOX) are iron-containing proteins, of which the first two are haemoproteins, we assessed the effects of inhibitors on the catalytic peroxidase properties of cyt *c*/CL complexes *in vitro*. Within the range of concentrations that correspond to the doses applied in our *in vivo* experiments, these inhibitors did not suppress the peroxidase activity (Supplementary Table 3). We found that the inhibitor cocktail partially decreased the levels of mono-oxygenated AA (AA_{ox}) and oxo-LA compared with the group of mice that received no drugs before irradiation (Supplementary Table 4). The production of dLA_{ox} did not appear to be affected by the mixture of inhibitors. This suggests that the generation of lipid mediators from CL/CL_{ox} is accomplished through enzymatic reactions distinct from the known Ca^{2+}-dependent mechanisms realized via the release of free fatty acids (FFAs) and their subsequent oxygenation.

Selective oxidation and hydrolysis of CL in the rat brain. In the rat brain, CLs were highly diversified and included mostly oxidizable polyunsaturated CLs (Fig. 2a). LC/MS analysis revealed that CCI caused depletion of oxidizable CLs that contain LA, AA and docosahexaenoic (DHA) acids (Fig. 2a) and formation of CL_{ox} (Fig. 2b) and its hydrolysis products: mCL (Fig. 2c) and FA_{ox} (Fig. 2d). CL_{ox} was mainly represented by species that contain one or two additional oxygen atoms (Fig. 2b). MS/MS analysis identified mono-oxygenated species of CL_{ox} with either LA_{ox} or AA_{ox} (Fig. 2b). mCLs were represented by non-oxidized as well as oxidized mCL_{ox} species (Fig. 2c and Supplementary Table 1 and Supplementary Fig. 3). The CL_{ox} content was lower than the amount of mCL: 0.10 ± 0.02 and 0.26 ± 0.08 pmol per nmol total phospholipids, respectively. In addition, the oxygenated species of non-esterified LA and AA were produced (Fig. 2d and Supplementary Fig. 4), whereby several lipid mediators were identified, such as 9-KODE, 13-KODE, 9-HODE, 13-HODE, 9-oxo-12,13-epoxyoctadecanoic acid (9,12,13-KEpOME), 9-HpODE, 13-HpODE, 12-HETE and 15-HETE (Supplementary Table 2). Markedly smaller amounts of oxygenated DHA were also detected (Fig. 2d). Quantitatively, the CCI-induced loss of CL species that contain PUFA was in good agreement with the accumulation of FA_{ox} (~5.1 and ~3.0 pmol per nmol total phospholipids, respectively). This indicates that CL can be a source of the CCI-induced production of FA_{ox}.

To ascertain whether the CL/CL_{ox}-dependent pathway may be cell-type specific, we compared the responses of two types of brain cells, cortical neurons and one of the major components of glia, astrocytes, to a standard treatment with H_2O_2 *in vitro*. We found that neurons (Supplementary Fig. 5 and Supplementary Table 5) contained more oxidizable polyunsaturated CL species than astrocytes (Supplementary Fig. 6 and Supplementary Table 5). Accordingly, the amounts and speciation of CL_{ox} after H_2O_2 exposure were also markedly richer in the cortical neurons than in the astrocytes (Supplementary Figs 5 and 6). Similarly, the levels and diversification of mCLs were also significantly greater in the former than in the latter (Supplementary Figs 5 and 6).

Generation of oxidized tetralinoleoyl cardiolipin ($TLCL_{ox}$) and its hydrolysis products in mitochondria. To characterize pathways of CL peroxidation and hydrolysis further, we utilized C57BL6 mouse heart and liver mitochondria in which CL was accountable for ~15% of the total phospholipids (Fig. 3). MS analysis demonstrated that oxidizable LA residues were present in all molecular species of CL (Supplementary Fig. 7). After exposure to a pro-oxidant, *t*-BuOOH, isolated mitochondria revealed the

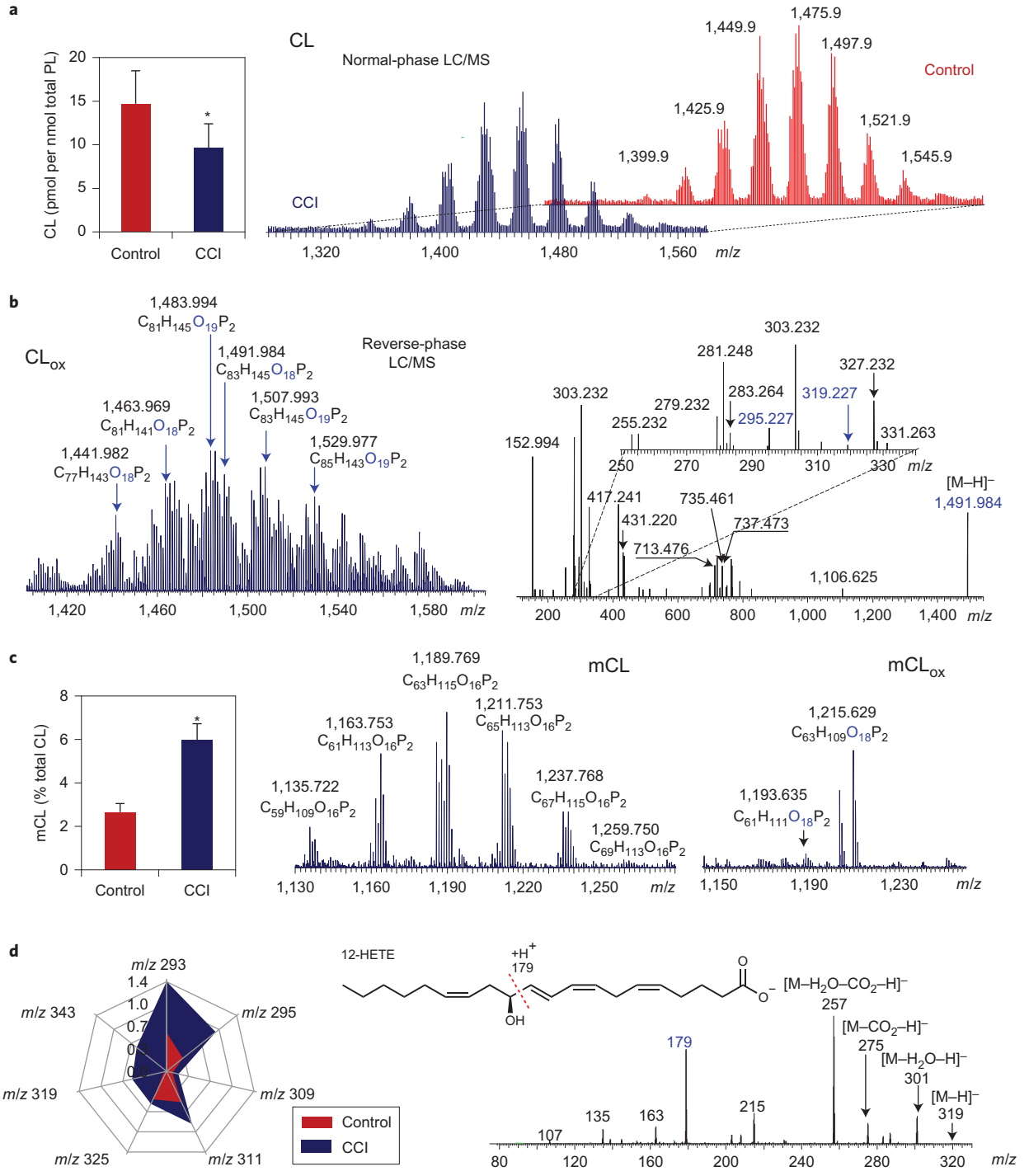

Figure 2 | Exposure of rats to CCI causes CL oxidation and accumulation of its hydrolysis products in the brain. a, Quantitation of polyunsaturated CL (left) and MS spectra of CL in the control and three hours after CCI (right). The spectrum of brain CLs includes nine major clusters of signals with 8–9 components of differing *m/z* in each. **b**, Typical MS spectrum of CL_{ox} (left) and fragmentation pattern of the CL_{ox} molecular ion with *m/z* 1,491.984 (right) represented by two species that contain either LA_{ox} (*m/z* 295.227) or AA_{ox} (*m/z* 319.227) and that originated from *m/z* 1,475.980. **c**, Quantitation of total mCL (left) and MS spectra of mCL (middle) and mCL_{ox} (right) formed after CCI. Dioxygenated species of mCL_{ox} were detected in injured brain. **d**, Quantitation of major polyunsaturated fatty acids (left) and MS/MS spectrum of molecular ion with *m/z* 319 (right). On the radar chart (left) data are presented as picomoles per nanomoles of total phospholipids. Species of LA_{ox} with *m/z* 293 (13-KODE, 9-KODE), *m/z* 295 (13-HODE, 9-HODE, 9,10-EpOME, 12,13-EpOME), *m/z* 311 (9-HpODE, 8,13-diHODE), *m/z* 309 (8,13-HKODE, 9,14-KHODE), *m/z* 325 (9,14-KHpODE, 9,14-HpKODE, 8,13-KHpODE, 8,13-HpKODE) and AA_{ox} with *m/z* 319 (12-HETE, 15-HETE) were identified. Small amounts of DHA_{ox} (*m/z* 343) were also detected. Data are means ± s.d., $^*P < 0.05$ versus control, $n = 4$.

same pattern of characteristic CL changes as *in vivo*: decreased amounts of oxidizable CLs (Fig. 3a), and accumulation of non-oxidized mCL (Fig. 3b) and LA_{ox} (containing one or two oxygens, respectively (Fig. 3c)).

Identification of cyt *c* as the catalyst of CL oxidation and hydrolysis. To assess directly the involvement of cyt *c* in CL peroxidation and hydrolysis products as a source of lipid mediators, we compared the production of mCL and FA_{ox} in cyt $c^{+/+}$ and

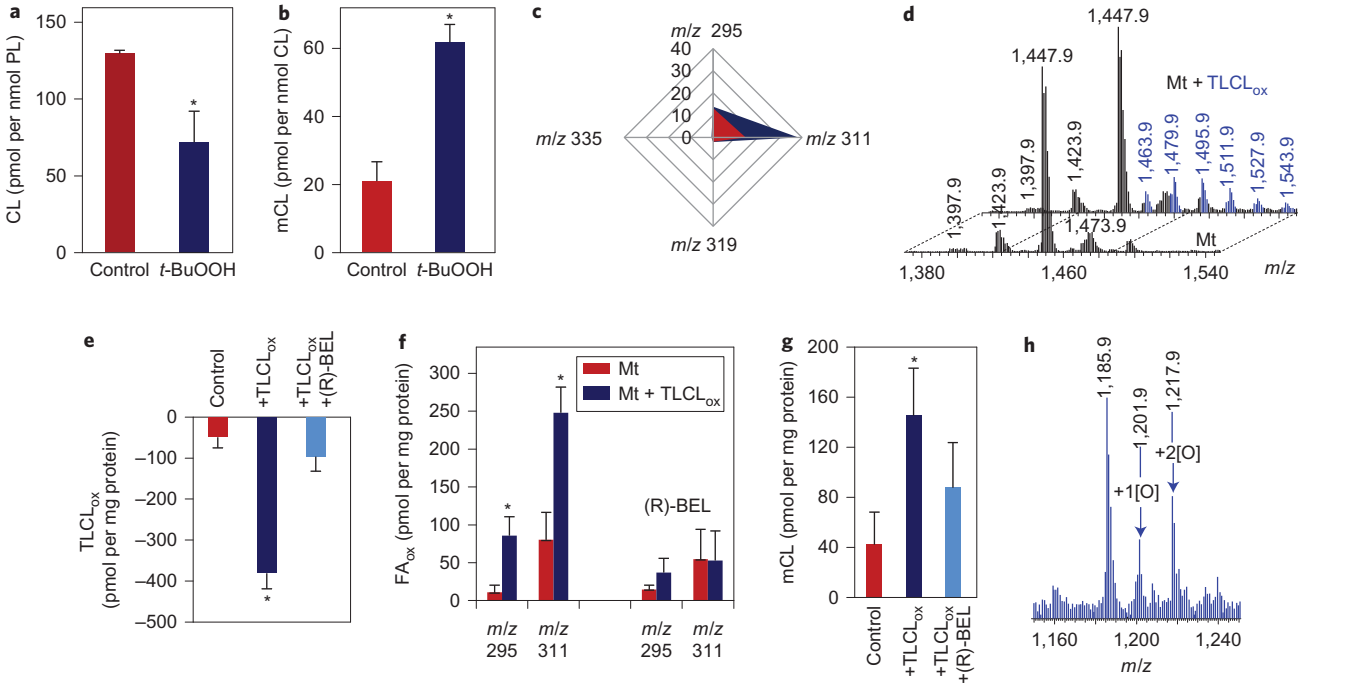

Figure 3 | Peroxidized CLs undergo phospholipase A_2-catalysed hydrolysis in mitochondria. a–c, Oxidation of CL (**a**) and accumulation of mCL (**b**) and FA_{ox} (**c**) in mouse heart mitochondria treated with *t*-BuOOH (150 μM). LA_{ox} (*m/z* 295 and 311) and LA_{ox} (*m/z* 319 and 335) that contained one or two oxygens were detected. Data are presented as picomoles FA_{ox} per nanomole phospholipids. Data are means ± s.d., $^*P < 0.05$ versus control, $n = 3$. **d–h**, The effect of (R)-BEL, the $iPLA_2\gamma$ inhibitor, on the hydrolysis of exogenous $TLCL_{ox}$ by mouse liver mitochondria: MS spectra of CL obtained from mouse liver mitochondria before and after the addition of $TLCL_{ox}$ (**d**). TLCL was oxidized by cyt c/H_2O_2 (see Supplementary Fig. 10) to give concentrations of $TLCL_{ox}$ (**e**), FA_{ox} (**f**) and mCL (**g**) in mitochondria incubated with exogenous $TLCL_{ox}$ in the presence and in the absence of (R)-BEL. **h**, MS spectrum of mCL from mitochondria incubated in the presence of $TLCL_{ox}$. Data are mean ± s.d., $^*P < 0.05$ versus non-treated mitochondria, $n = 3$.

cyt $c^{-/-}$ mouse embryonic cells (MECs) during apoptosis triggered by non-oxidant (actinomycin D (ActD)) or oxidant (*t*-BuOOH) stimuli (Fig. 4a). No significant differences were found in the total content and molecular speciation of CLs in cyt $c^{+/+}$ and cyt $c^{-/-}$ cells (approximately 3% total phospholipids; 31.1 ± 4.9 and 33.7 ± 7.1 pmol CL per nmol total phospholipids, respectively) (Fig. 4b and Supplementary Fig. 8). Treatment with ActD or *t*-BuOOH caused a significant decrease of oxidizable polyunsaturated species of CL and accumulation of CL_{ox} species with one or two oxygens in cyt $c^{+/+}$ cells (but not in cyt $c^{-/-}$ cells) (Fig. 4b and Supplementary Fig. 8). Quantitatively, the amounts of CL_{ox} produced in cyt $c^{+/+}$ cells challenged with either ActD or *t*-BuOOH increased 2.6 and 3.0 times compared to those of untreated controls. Analysis of the hydrolysis products revealed the presence of both oxidized and non-oxidized mCL (Fig. 4c) as well as of LA_{ox} (Fig. 4d). Mono- and dioxygenated molecular species of mCL_{ox} were the predominant forms to accumulate in the cells on the treatments (Fig. 4c). mLA_{ox} was the main product in ActD-treated cyt $c^{+/+}$ cells, represented by a mixture of 9-HODE and 13-HODE (Fig. 4d). No significant increase in the levels of CL_{ox} and CL hydrolysis products was detected in ActD- and *t*-BuOOH-treated cyt $c^{-/-}$ cells (Fig. 4). ActD and *t*-BuOOH triggered apoptosis in cyt $c^{+/+}$ cells, as evidenced by a marked increase of PS externalization (Fig. 4a), whereas these pro-apoptotic effects were not found in cyt $c^{-/-}$ cells[11].

MECs express two isoforms of cyt *c*, somatic (s-cyt *c*) and testicular (t-cyt *c*)[21–23]. Western-blot analysis established that t-cyt *c* accounted for ~45% of the total cyt *c* in MECs (Supplementary Fig. 9). In cyt $c^{-/-}$ cells, the amount of t-cyt *c* was ~1.5 times lower than that in cyt $c^{+/+}$ cells (0.83 ± 0.05 and 1.24 ± 0.08 ng per microgram protein, respectively). As cyt $c^{-/-}$ cells rely more on glycolysis than on mitochondrial respiration for ATP generation[24] they maintain lower levels of mitochondria. Indeed, western blots showed that the levels of several mitochondrial marker proteins (COX-IV, MnSOD, TIM23) were ~46–83% lower in cyt $c^{-/-}$ cells versus cyt $c^{+/+}$ cells (Supplementary Fig. 9). Short-interfering RNA knockdown of the t-cyt *c* in cyt $c^{-/-}$ cells to ~50% of its content (Supplementary Fig. 9) did not affect the already low level of CL oxidation after ActD treatment. Similar to cyt $c^{-/-}$ cells, the low level of mCL in cyt $c^{-/-}$ with knockdown t-cyt *c* remained unchanged after ActD exposure. These data suggest that t-cyt *c* is not a significant contributor to the generation of CL-driven lipid mediators.

Hydrolysis of $TLCL_{ox}$ by mitochondrial Ca^{2+}-$iPLA_2\gamma$. $iPLA_2\gamma$ has been suggested as a probable candidate catalyst capable of hydrolysing oxidized phospholipids in mitochondria[25]. To assess its role in the hydrolysis of CL_{ox} species, we biosynthesized (using a cyt c/H_2O_2 system) and purified (to the level of 99% using LC/MS) $TLCL_{ox}$ with 1–8 oxygens in four LA residues (see Supplementary Table 6 and Supplementary Fig. 10) and analysed the products formed in the presence of a specific $iPLA_2\gamma$ inhibitor, (R)-BEL, in rat liver mitochondria (Fig. 3d). Mitochondria effectively hydrolysed $TLCL_{ox}$ as evidenced by (1) the decrease of $TLCL_{ox}$ content (Fig. 3e) and (2) the accumulation of LA_{ox} (with one or two oxygens) (Fig. 3f) as well as non-oxidized mCL and mCL_{ox} (Fig. 3g,h). The hydrolysis of $TLCL_{ox}$ was effectively blocked by (R)-BEL (Fig. 3).

Hydrolysis of $TLCL_{ox}$ by PAF acetylhydrolase. Mitochondria with externalized CL and/or CL_{ox} as well as cyt *c* can be released into the circulation during an injury and/or disease process[26]. Thus, circulating CL and CL_{ox} can be a source of lipid mediators as well. Several phospholipases, including lipoprotein-associated PLA_2

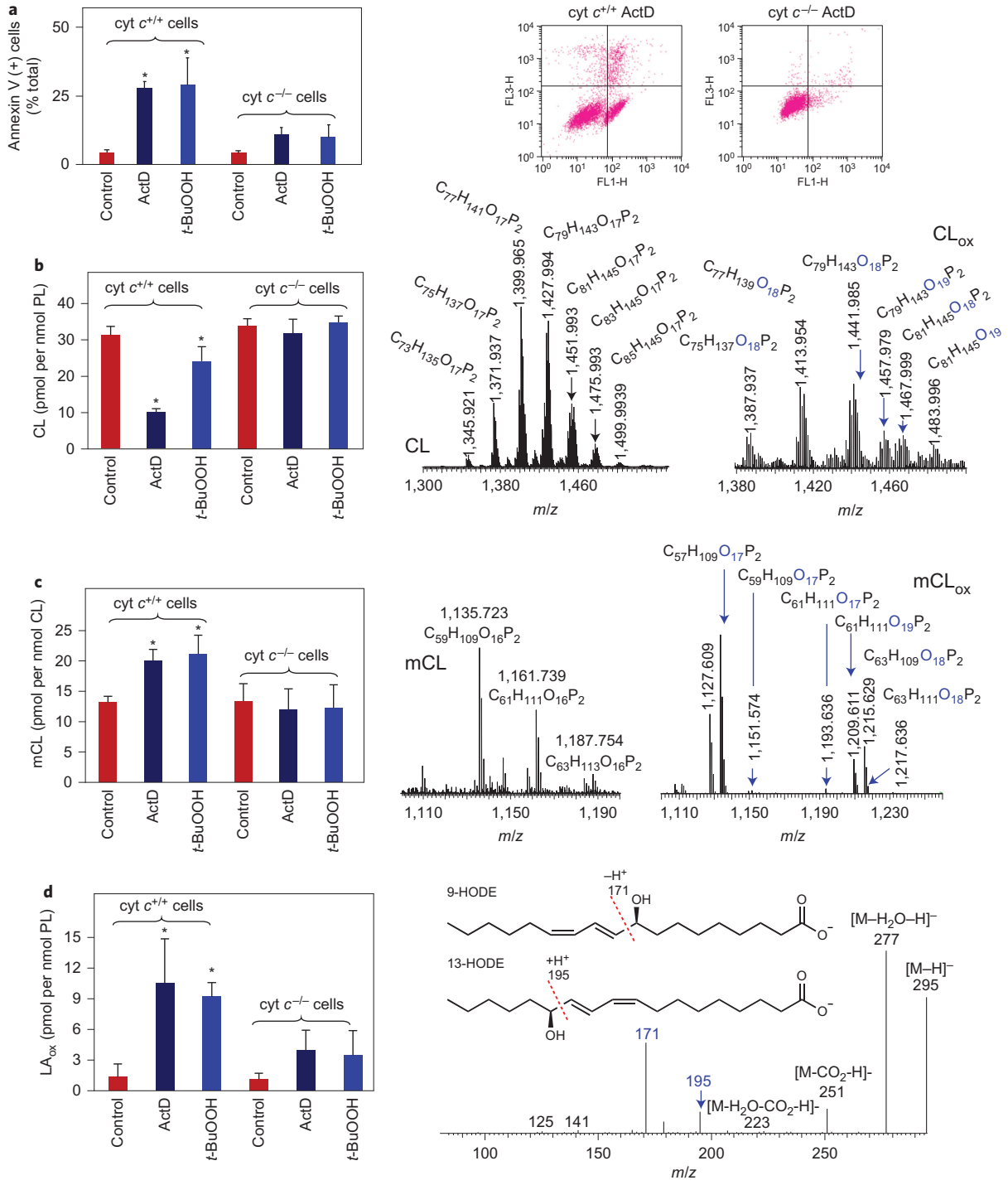

Figure 4 | Execution of apoptosis is accompanied by CL oxidation and accumulation of its hydrolysis products in mouse embryonic cyt $c^{+/+}$ (but not cyt $c^{-/-}$) cells. a, Assessments of a biomarker of apoptosis, externalized phosphatidylserine, in cyt $c^{+/+}$ and cyt $c^{-/-}$ cells by annexin V binding (left). On the right are flow cytometry data from a representative experiment after the treatment of cells with ActD (100 ng ml^{-1}, 16 hours): the number of annexin V/FITC-positive cells is shown in log scale. **b**, Consumption of CL in either ActD- or *t*-BuOOH-treated (200 μM, 16 hours) cyt $c^{+/+}$ and cyt $c^{-/-}$ cells (left), and MS spectra of CL (middle) and CL_{ox} (right) from cyt $c^{+/+}$ cells exposed to ActD. **c**, Accumulation of mCL in either ActD- or *t*-BuOOH-treated cyt $c^{+/+}$ and cyt $c^{-/-}$ cells (left), and MS spectra of mCL (middle) and mCL_{ox} (right) from cyt ActD-treated $c^{+/+}$ cells. **d**, Accumulation of LA_{ox} in ActD- and *t*-BuOOH-treated cyt $c^{+/+}$ and cyt $c^{-/-}$ cells (left), and MS/MS fragmentation pattern of LA_{ox} (*m/z* 295) (right) formed in ActD-treated cyt $c^{+/+}$ cells. mLA_{ox} was accumulated predominantly and represented by both 9-HODE and 13-HODE. Data are mean ± s.d., $^*P < 0.01$ versus control, $n = 3$–4.

($LpPLA_2$) or platelet activating factor acetylhydrolase (PAF-AH), have been shown to hydrolyse oxidatively modified phospholipids selectively to liberate FA_{ox}[27]. Recently, we identified oxidized PS as a good substrate for $Lp\text{-}PLA_2$[28]. As TLCL is the most-predominant species of CL in circulation, we tested the ability of PAF-AH to release oxygenated FAs from $TLCL_{ox}$ produced in a cyt *c*-driven reaction (Supplementary Fig. 10). LC/MS analysis revealed the accumulation of mCL that contained both LA and LA_{ox} (Fig. 5a–c), whereby LA_{ox} was represented by molecular species with one or two oxygens (Fig. 5d). A markedly less-effective hydrolysis was

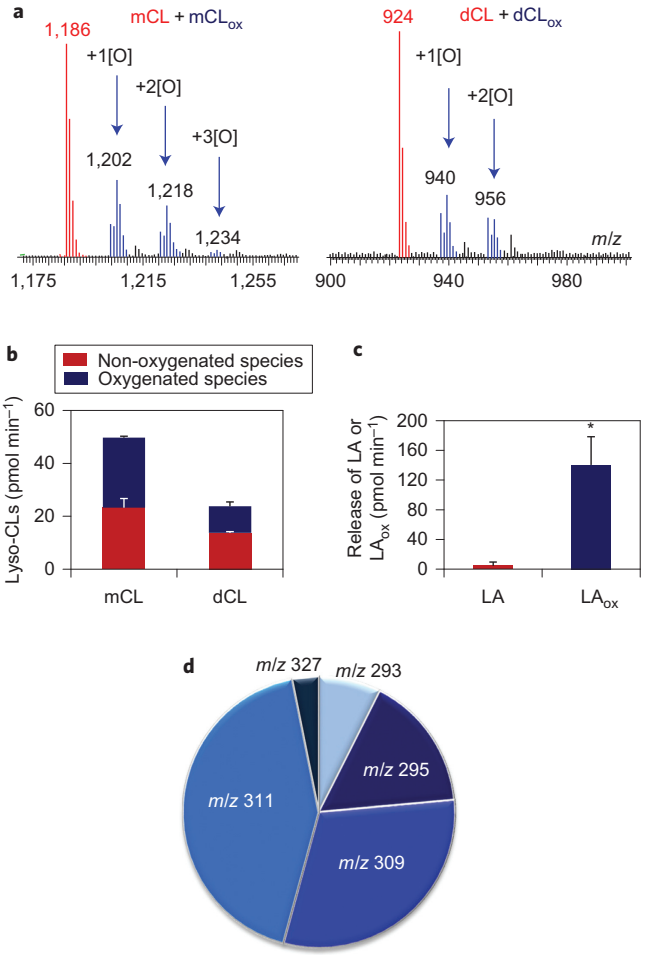

Figure 5 | PAF-AH catalyses hydrolysis of $TLCL_{ox}$. **a**, MS spectra of mCLs (left) and dCLs (right) formed during PAF-AH-driven hydrolysis of oxygenated $TLCL_{ox}$. Arrows show mCL_{ox} and dCL_{ox} species (and their *m/z* values) with indicated oxygen atoms added. **b**,**c**, Quantitative assessment of lyso-CLs (**b**), and non-oxygenated and oxygenated LA (**c**) formed during PAF-AH-driven hydrolysis of $TLCL_{ox}$. **d**, Identification and quantification of LA_{ox} liberated after hydrolysis of $TLCL_{ox}$ by PAF-AH. Molecular ions of LA_{ox} with *m/z* 293 (13-KODE, 9-KODE), *m/z* 295 (13-HODE, 9-HODE, 9,10-EpOME, 12,13-EpOME), *m/z* 309 (8,13-HKODE, 9,14-KHODE), *m/z* 311 (9-HpODE, 13-HpODE and 8,13-DiHODE) and *m/z* 327 (9,12,13-HpEpOME) were detected. Data are means ± s.d., $^*P < 0.05$ versus LA, $n = 4$.

detected when non-oxidized TLCL was treated with PAF-AH (data not shown). Thus, PAF-AH predominantly hydrolyses oxygenated molecular species of CL to generate lipid signalling molecules formed in cyt *c*-catalysed reactions.

Diversity of oxygenated FAs after hydrolysis of brain CL_{ox} generated by cyt c/H_2O_2. The high diversification and enrichment with PUFA of brain lipids makes neuro-CLs particularly interesting as a source of lipid mediators generated via CL oxidation by cyt *c*. Indeed, we identified 56 major molecular species of CL in lipid extracts from the mouse brain (Supplementary Table 7), of which 55 were highly oxidizable polyunsaturated CLs that contained 1–4 PUFAs (Fig. 6a). To establish the molecular identity and stereospecificity of peroxidizable PUFAs in neuro-CLs we employed a mixture of PLA_1 with PLA_2 and established that the dominant PUFAs of CL were represented by AA and LA (Fig. 6a). DHA, eicosapentaenoic, eicosatrienoic and octadecatrienoic acids were detected as well, but in relatively lower abundance. Cyt c/H_2O_2 caused significant decreases of PUFA-containing molecular species of CL (Fig. 6b,c). By employing PLA_1 plus PLA_2 as a tool to liberate fatty acid (FA) from both *sn*-1 and *sn*-2 positions of CL_{ox}, we identified (using MS/MS analysis) highly diversified molecular species of LA_{ox} and AA_{ox} (Fig. 6d), which included those detected in acutely injured tissues (the brain after CCI and the small intestine after WBI (Supplementary Table 2)) as well as in apoptotic cyt $c^{+/+}$ cells. In addition, oxidatively truncated FA molecular species were detected (Supplementary Table 2). Overall, 31 molecular species of FA_{ox} were identified as the products of brain CL_{ox} hydrolysis.

Peroxidation of TLCL/cyt *c* complexes is Ca^{2+} independent. The conventional pathways for the generation of lipid mediators are regulated by Ca^{2+} because of the highly Ca^{2+}-dependent PLA_2-driven release of PUFA from phospholipids[29]. Both PAF-AH and $iPLA_2\gamma$ in mitochondria do not require Ca^{2+} for their activation. To ascertain whether the entire process of the cyt *c*-initiated generation of lipid mediators from CL is Ca^{2+} independent we examined the effects of Ca^{2+} on the peroxidase activity of TLCL/cyt *c* complexes *in vitro*. Ca^{2+} did not cause any increase in the peroxidase activity of complexes towards a prototypical phenolic substrate, AmplexRed or TLCL oxidation (Supplementary Fig. 11).

Discussion

Oxygenated free PUFAs (generated by a wide array of enzymes, including COX-1 and COX-2, lipoxygenases (5-LOX, 12-LOX and 15-LOX) and cytochrome P450 isoforms (reviewed in Rouzer and Marnett[5] and Stables *et al.*[7])) have numerous physiological roles. The potent biological effects of lipid regulators necessitate the maintenance of very low endogenous levels of free PUFA. As a result, their availability is the rate-limiting step in the generation of lipid mediators[4]. Release of PUFA precursors from their phospholipid storage sites is achieved via the action of Ca^{2+}-dependent PLA_2 (ref. 30). We report a new Ca^{2+}-independent pathway for the selective generation of lipid mediators from a mitochondria-specific phospholipid, CL, whereby oxidation of FA residues is catalysed by an intermembrane-space protein, cyt *c*, directly in the esterified phospholipid. This is followed by hydrolysis of CL_{ox} species by two types of PLA_2 specific to oxidatively modified phospholipids. This novel pathway disobeys the major dogmas of lipid-mediator biochemistry with regards to (1) oxygenation of a phospholipid rather than a FFA as the reaction substrate, (2) mitochondrial, rather than cytosolic, localization, (3) an electron carrier cyt *c*, rather than an oxidase, as the reaction catalyst, (4) the final, rather than the initial, hydrolytic stage using CL_{ox} species by PLA_2 to synthesize oxygenated PUFA ($PUFA_{ox}$) and (5) the Ca^{2+}-independent, rather than the Ca^{2+}-dependent, nature of the pathway.

One can predict specific features of the regulation of CL-dependent process that are markedly different from the 'conventional' biosynthesis of oxygenated lipid mediators. The mitochondrial pathway is strictly dependent on the catalytic interactions between cyt *c* and CL. However, these two participants have limited access to each other. The former is confined to the intermembrane space and the latter is 'cloaked' almost exclusively in the IMM[31]. Importantly, ~15% of cyt *c* is believed to be hydrophobically bound to the IMM, probably via its binding to CL in the outer leaflet of the IMM, and cannot be removed from mitochondria, as occurs for the majority of cyt *c* on treatment with solutions of high ionic strength[32]. The function of the tightly membrane-bound cyt *c* in normal mitochondria has not been identified. Given that CL-bound cyt *c* cannot act as an electron acceptor from respiratory complex III[33], we speculate that catalysis of the

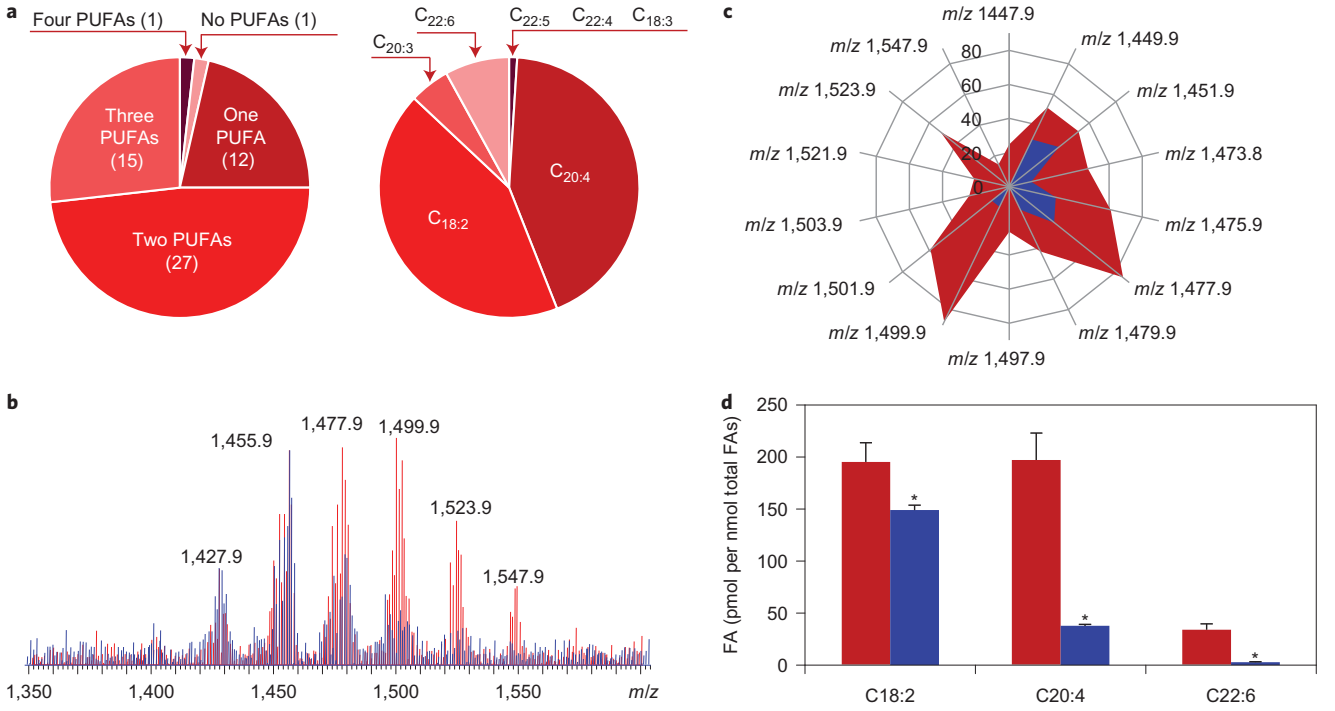

Figure 6 | Cyt c/H_2O_2 induces oxidation of PUFA residues of CL isolated from mouse brain. a, Characterization of PUFA esterified to brain CL with the number of CL molecular species that contain PUFA (left), and PUFA distribution in brain CL species (right). **b**,**c**, MS spectra (**b**) and quantitative assessment of brain CL molecular species (**c**) obtained before (red) and after (blue) treatment with cyt *c* in the presence of H_2O_2. **d**, Quantitative assessment of PUFA of non-oxygenated CL (red) and CL exposed to cyt c/H_2O_2 (blue). $^*P < 0.05$ versus control (CL not treated with cyt *c*). Data are means ± s.d., $n = 3$.

CL-dependent formation of lipid mediators may represent an unrecognized function of cyt *c*.

For the peroxidase activity of cyt *c*/CL complexes, the presence of sufficient amounts of oxidizing equivalents, such as H_2O_2 or lipid hydroperoxides ('peroxide tone'[34,35]), is essential to trigger CL oxidation. Their supply may be driven by disrupted electron transport, which probably occurs as a consequence of cyt *c* binding with CL[34]. The complex has a redox potential ~400 mV more negative than that of the free cyt *c*, an effect that precludes cyt *c*'s function as an electron acceptor from mitochondrial complex III[33]. As a result, accumulating reduced intermediates serves to donate electrons to molecular oxygen to yield superoxide radicals. Spontaneous or catalysed dismutation of the latter generates H_2O_2 that feeds the catalytic peroxidase cycle of cyt *c*/CL complexes. This dependency on H_2O_2 as the source of oxidizing equivalents disappears with the accumulation of FA hydroperoxides or CL hydroperoxides that can act as more-efficient substrates for the peroxidase half-cycle of the process[35].

Cells can express, at different proportions, two isoforms of cyt *c*, s-cyt *c* and t-cyt *c*[21–24]. We found that t-cyt *c* does not contribute significantly to the production of lipid mediators. To investigate whether there are potential differences in s-cyt *c* versus t-cyt *c* participation in lipid oxidation, we compared the interaction of two isoforms of cyt *c* with CL using sequence analysis, molecular structural modelling, and molecular docking and computational simulations. The sequences of s- and t-cyt *c* and three-dimensional (3D) structures displayed a high similarity (Supplementary Fig. 12). Further, ligand-docking analysis revealed a close similarity between the two isoforms in binding a typical peroxidation substrate, TLCL, as judged by closely matching predicted binding-energy values (Supplementary Table 8). Finally, coarse-grained molecular dynamics simulations of cyt *c* interactions with lipid bilayers revealed equally avid binding to TLCL-containing membranes at the early stages in the simulation and lack thereof with lipid bilayers devoid of TLCL (Supplementary Fig. 12). This suggests that t-cyt *c*, like s-cyt *c*, should be competent towards peroxidase functions, including CL peroxidation.

The failure of t-cyt *c* to operate as a catalyst of CL oxidation in MECs may arise mostly because of its presence as an apoprotein whereby its biosynthesis into the catalytically active holoenzyme may be the limiting factor. According to Kim *et al.*, three times more t-cyt *c* was detected by radioimmunoassay than by spectral assessments of the catalytically competent haemoprotein[36]. However, the anti-t-cyt *c* antibody employed in our study does not distinguish between the apo- and holoproteins. Differences in the localization of these two isoforms of cyt *c* in the intermembrane space and their differential interactions with CLs and other proteins may also be contributory to their dissimilar peroxidase activity towards CLs[37,38]. The suggested higher pro-apoptotic activity of t-cyt *c* versus s-cyt *c* may be realized through their differential interactions with procaspase complexes (Apaf) and the formation of apoptosomes[39].

An important feature of cyt *c*-catalysed oxygenation reactions described in this work is not only the accumulation of the expected hydroperoxy-CL and hydroxy-CL[5], but also the presence of epoxy- and oxoderivatives and truncated products of oxidative cleavage. Whether these derivatives are produced by an enzymatic cyt *c*-catalysed reaction or a non-enzymatic process caused by degradation and release of cyt *c*'s haem is unknown. Similar products require additional enzymatic activities (that is, epoxidase and epoxide hydrolases) in the traditional pathways triggered by COX and LOX[5]. Our results with pharmacological inhibitors of two different pathways, COX/LOX/P450 and (R)-BEL, support a role for CL oxidation as a source of the generated lipid mediators. In line with our data, disturbed CL reacylation in mice with knockdown tafazzin (modelling the Barth syndrome) was accompanied by the altered pattern of HETE and oxidized LA and DHA metabolites[40].

The final step in the biosynthesis of oxygenated FFAs requires hydrolysis of oxidatively modified CLs by PLA_2. Several representatives from different groups of secretory PLA_2 of a large superfamily

of PLA_2 were shown to display hydrolysing activity towards peroxidized phospholipids (reviewed in David *et al.*[29]). Among these, the best studied is $LpPLA_2$ (a Ca^{2+}-independent $LpPLA_2$ or type VIIA PLA_2), which can be represented by intracellular and secreted forms[30] and is active towards oxygenated long-chain and truncated forms of phosphatidylcholine[41]. Oxidized PS has been identified as a representative of anionic peroxidized phospholipids readily hydrolysable by Lp-PLA_2[28].

CLs have been identified as signalling molecules in two major biological functions: mitophagy[42] and apoptosis[11]. In both cases, CL is externalized to the mitochondrial surface, which suggests that any injury to plasma membrane may be associated with the release of these 'CL-decorated' mitochondria into extracellular environments. Assuming that apoptosis commonly transitions to necrosis, mitochondria may (with their externalized CL and CL_{ox}) act as damage-associated molecular patterns[26,43]. Our studies reveal that not only CL and CL_{ox}, but also CL_{ox} hydrolysis products (mCL and FFA_{ox}) may be released, along with mitochondria, from injured cells. Importantly, sufficient hydrophobicity of mCL retains its association with mitochondria. However, oxygenated mCLs may lose their association with the OMM and partition into the aqueous phase of extracellular compartments. Oxygenated FFAs are also water soluble, and hence diffuse independently of mitochondrial surfaces. Releases of CL[44] and cyt *c*[45] from injured host cells into the extracellular space have been shown. Thus lipid mediators may also be generated extracellularly from CL with the contribution of cyt *c* and subsequent hydrolysis of CL_{ox} by Lp-PLA_2. Overall, CL-dependent lipid mediators may be represented by a diversified variety of membrane-associated and freely diffusible and circulating signalling molecules, the identification and quantitative analysis of which will represent an intriguing opportunity for future studies.

The brain has an unprecedented diversification of CLs[13]. By using brain CLs, we showed that a significant variety of lipid mediators could be generated by cyt *c*-catalysed oxygenation processes. In fact, we found that all eight well-known LA-based lipid mediators were generated by cyt *c*/H_2O_2 (Supplementary Table 2). In the AA series, we were able to identify nine species of lipid mediators (Supplementary Table 2). A relatively smaller number of oxygenated derivatives of docosapentaenoic acid and DHA were detected in spite of the significant proportion of these FA residues in brain CLs. Also, terminally hydroxylated metabolites of AA, including 17-HETE, 18-HETE, 19-HETE and 20-HETE, were not found, which implies that terminal hydroxylation reactions are not catalysed by cyt *c*/H_2O_2 and are probably formed enzymatically after AA liberation.

The ranking order of FA residue oxidation in the model biochemical system, in which all the CL substrates are equally available, was DHA > AA ≫ LA. The amounts of DHA, AA and LA decreased almost 20-, 5- and 0.3-fold, respectively. The energies for hydrogen abstraction in the α-position to bis-allylic double bonds for different FAs with multiple double bonds decrease in the order LA < AA < DHA. Accordingly, the propagation rate constants for FA oxidation determined for LA (one bis-allylic group), AA (three bis-allylic groups), EPA (four bis-allylic groups) and DHA (five bis-allylic groups) increase at ratios of 1, 3.2, 4.0 and 5.4 (ref. 46). This is consistent with the assumption that hydrogen abstraction is essential for the oxidation of different polyunsaturated species of CLs by cyt *c*'s protein-immobilized Tyr radical: $Tyr\text{-}O^{\bullet} + CL\text{–}H \rightarrow Tyr\text{–}OH + CL^{\bullet}$. Thus, preferential oxidation of LA in brain CL's *in vivo* does not correlate with the chemical reactivity, which suggests that CL oxidation in mitochondria is not a simple reaction of CLs with cyt *c*. The availability of CLs for oxidation by cyt *c* in the intermembrane space probably defines the specificity of the reaction towards different CL species. Our findings with brain CLs may provide a long-awaited explanation for the well-known large variety of CL species in the brain and some other tissues (for example, the small intestine and lung), as the findings imply that the CL species are used as the precursors for the biosynthesis of diversified lipid mediators[47].

In conclusion, we describe a new pathway for the generation of lipid mediators. This novel Ca^{2+}-independent pathway localizes to mitochondria, involves cyt *c*-catalysed oxygenation of CL-esterified PUFA residues and is followed by hydrolysis of CL_{ox} species by two types of $iPLA_2$ specific towards oxidatively modified phospholipids.

Methods

This section describes key experiments only; an extended experimental section is provided in the Supplementary Methods.

CCI. CCI to the left parietal cortex in 17-day-old rats was performed as described previously[48]. For all studies, a 6 mm metal pneumatically driven impactor tip was used. The velocity of the impact was 4.0 ± 0.2 m s^{-1}, with a penetration depth of 2.5 mm.

WBI. C57BL/6NHsd female mice were irradiated with a dose of 10 Gy using a J. L. Shepherd Mark 1 Model 68 caesium irradiator at a dose rate of 80 cGy min^{-1}, as described previously[49]. (A dose of 10 Gy WBI is $LD_{100/30}$ for C56Bl6 mice, which means this dose causes death of all animals within 30 days after the exposure.) Irradiated mice were euthanized 10 or 24 hours later by CO_2 inhalation. All procedures were approved by the Institutional Animal Care and Use Committee of the University of Pittsburgh and performed according to the protocols established.

Analysis of CL and mCL molecular species. This was performed using a Dionex Ultimate 3000 HPLC system coupled on-line to a linear ion-trap mass spectrometer (LXQ, ThermoFisher Scientific) using a Luna 3 μm Silica (2) 100 Å column (Phenomenex), as described previously[28]. To analyse oxygenated species, CL and mCL were isolated from total lipids by normal-phase 2D-HPTLC using mobile phases, as described by Rouser *et al.*[50]. To prevent lipid oxidation during separation, chromatography was performed under N_2 conditions on silica plates (5 × 5 cm, Whatman) treated with diethylenetriaminepentaacetic acid. CL and mCL were extracted from silica spots[49] and used for reverse-phase electrospray ionization (ESI)-LC/MS analysis. LC/MS analysis was performed using a Dionex Ultimate 3000 RSLCnano system coupled on-line to a Q-Exactive hybrid quadrupole-orbitrap mass spectrometer (ThermoFisher Scientific) using a C_8 column (Luna 3 μm, 100 Å, 150 × 2 mm (Phenomenex)). For CL_{ox} an isocratic solvent system that consisted of 2-propanol/water/triethylamine/acetic acid, 45:5:0.25:0.25 v/v, was delivered at 150 μl min^{-1} for 20 minutes. For mCL_{ox}, a gradient of solvents A (acetonitrile/water/triethylamine/acetic acid, 45:5:0.25:0.25 v/v) and B (2-propanol/water/triethylamine/acetic acid, 45:5:0.25:0.25 v/v) was used at a flow rate of 150 μl min^{-1} as follows: 0–10 minutes isocratic at 50% solvent B, 10–20 minutes linear gradient from 50 to 100% solvent B, 20–32 minutes isocratic at 100% solvent B, 32–35 minutes linear gradient from 100 to 50% solvent B and 35–45 minutes isocratic at 50% solvent B. Spectra were acquired in negative-ion mode using a spray voltage of 4.0 kV and a capillary temperature of 320 °C. Scans were acquired in data-dependent mode with an inclusion list for both CL/CL_{ox} and mCL/mCL_{ox} species, isolation width of 1.0 Da and normalized collision energy of 24 in high-energy collisional dissociation mode. TMCL-$(14:0)_4$ (Avanti Polar Lipids Inc.) and mCL-$(14:0)_3$ were used as internal standards. Peaks with a signal-to-noise ratio of three and higher were taken into consideration.

Detection of oxidized FA. LA_{ox} was analysed by LC/MS using a Dionex Ultimate 3000 HPLC system coupled on-line to a LXQ linear ion-trap mass spectrometer (ThermoFisher Scientific). A C_{18} column (Luna, 3 μm, 150 × 2 mm (Phenomenex)) and gradient solvents (A, tetrahydrofuran/methanol/water/CH_3COOH, 25:30:50:0.1 v/v; B: methanol/water 90:10 v/v) that contained 5 mM ammonium acetate were used. The column was eluted at a flow rate of 0.2 ml min^{-1} during first the three minutes isocratically at 50% B, from three to 23 minutes with a linear gradient from 50 to 98% solvent B, then 23–40 minutes isocratically using 98% solvent B, 40–42 minutes with a linear gradient from 98 to 50% solvent B and 42–28 minutes isocratically using a 50% solvent B for equilibration of the column. Spectra were acquired in negative-ion mode using a spray voltage of 5.0 kV and a capillary temperature of 150 °C. The assay method for quantitative assessment of free AA_{ox} and DHA_{ox} was carried out as previously described by Miller *et al.*[51]. Briefly, LC was performed using an acuity ultra-performance LC autosampler (Waters). Separation of analytes was conducted on a UPLC BEH C_{18}, 1.7 μm (2.1 × 100 mm) column. A gradient mobile phase of 0.005% acetic acid, 5% acetonitrile in deionized water and 0.005% acetic acid in acetonitrile was used with a run time of 6.4 minutes. Analysis was performed using a TSQ Quantum Ultra (ThermoFisher Scientific) triple quadrupole mass spectrometer with heated ESI in the negative selective reaction monitoring mode. Analytical data were acquired and analysed using Xcalibur software.

Received 15 July 2013; accepted 16 March 2014; published online 20 April 2014

References

1. Murphy, M. P. Modulating mitochondrial intracellular location as a redox signal. *Sci. Signaling* **5,** pe39 (2012).
2. Bozza, P. T., Bakker-Abreu, I., Navarro-Xavier, R. A. & Bandeira-Melo, C. Lipid body function in eicosanoid synthesis: an update. *Prostaglandins Leukot. Essent. Fatty Acids* **85,** 205–213 (2011).
3. Gutierrez, J., Ballinger, S. W., Darley-Usmar, V. M. & Landar, A. Free radicals, mitochondria, and oxidized lipids: the emerging role in signal transduction in vascular cells. *Circ. Res.* **99,** 924–932 (2006).
4. Perez-Chacon, G., Astudillo, A. M., Balgoma, D., Balboa, M. A. & Balsinde, J. Control of free arachidonic acid levels by phospholipases A2 and lysophospholipid acyltransferases. *Biochim. Biophys. Acta* **1791,** 1103–1113 (2009).
5. Rouzer, C. A. & Marnett, L. J. Endocannabinoid oxygenation by cyclooxygenases, lipoxygenases, and cytochromes P450: cross-talk between the eicosanoid and endocannabinoid signaling pathways. *Chem. Rev.* **111,** 5899–5921 (2011).
6. Serhan, C. N., Chiang, N. & Van Dyke, T. E. Resolving inflammation: dual anti-inflammatory and pro-resolution lipid mediators. *Nature Rev. Immunol.* **8,** 349–361 (2008).
7. Stables, M. J. & Gilroy, D. W. Old and new generation lipid mediators in acute inflammation and resolution. *Prog. Lipid Res.* **50,** 35–51 (2011).
8. Rice, G. E. Secretory phospholipases and membrane polishing. *Placenta* **19,** 13–20 (1998).
9. Vance, J. E. & Tasseva, G. Formation and function of phosphatidylserine and phosphatidylethanolamine in mammalian cells. *Biochim. Biophys. Acta* **1831,** 543–554 (2013).
10. Wright, M. M., Howe, A. G. & Zaremberg, V. Cell membranes and apoptosis: role of cardiolipin, phosphatidylcholine, and anticancer lipid analogues. *Biochem. Cell Biol.* **82,** 18–26 (2004).
11. Kagan, V. E. *et al.* Cytochrome *c* acts as a cardiolipin oxygenase required for release of proapoptotic factors. *Nature Chem. Biol.* **1,** 223–232 (2005).
12. Rouzer, C. A. & Marnett, L. J. Cyclooxygenases: structural and functional insights. *J. Lipid Res.* **50,** S29–S34 (2009).
13. Bayir, H. *et al.* Selective early cardiolipin peroxidation after traumatic brain injury: an oxidative lipidomics analysis. *Ann. Neurol.* **62,** 154–169 (2007).
14. Tyurin, V. A. *et al.* Mass-spectrometric characterization of phospholipids and their primary peroxidation products in rat cortical neurons during staurosporine-induced apoptosis. *J. Neurochem.* **107,** 1614–1633 (2008).
15. Yin, H. *et al.* Role of mitochondria in programmed cell death mediated by arachidonic acid-derived eicosanoids. *Mitochondrion* **13,** 209–224 (2013).
16. Saab-Aoude, S., Bron, A. M., Creuzot-Garcher, C. P., Bretillon, L. & Acar, N. A mouse model of *in vivo* chemical inhibition of retinal calcium-independent phospholipase A2 (iPLA2). *Biochimie* **95,** 903–911 (2013).
17. Imig, J. D., Falck, J. R. & Inscho, E. W. Contribution of cytochrome P450 epoxygenase and hydroxylase pathways to afferent arteriolar autoregulatory responsiveness. *Br. J. Pharmacol.* **127,** 1399–1405 (1999).
18. Liu, H. *et al.* Increased generation of cyclopentenone prostaglandins after brain ischemia and their role in aggregation of ubiquitinated proteins in neurons. *Neurotoxicity Res.* **24,** 191–204 (2013).
19. Rifkind, A. B., Lee, C., Chang, T. K. & Waxman, D. J. Arachidonic acid metabolism by human cytochrome P450s 2C8, 2C9, 2E1, and 1A2: regioselective oxygenation and evidence for a role for CYP2C enzymes in arachidonic acid epoxygenation in human liver microsomes. *Arch. Biochem. Biophys.* **320,** 380–389 (1995).
20. Laufer, S. A., Augustin, J., Dannhardt, G. & Kiefer, W. (6,7-diaryldihydropyrrolizin-5-yl)acetic acids, a novel class of potent dual inhibitors of both cyclooxygenase and 5-lipoxygenase. *J. Med. Chem.* **37,** 1894–1897 (1994).
21. Narisawa, S. *et al.* Testis-specific cytochrome *c*-null mice produce functional sperm but undergo early testicular atrophy. *Mol. Cell. Biol.* **22,** 5554–5562 (2002).
22. Vempati, U. D. *et al.* Role of cytochrome *c* in apoptosis: increased sensitivity to tumor necrosis factor alpha is associated with respiratory defects but not with lack of cytochrome *c* release. *Mol. Cell. Biol.* **27,** 1771–1783 (2007).
23. Vempati, U. D., Han, X. & Moraes, C. T. Lack of cytochrome *c* in mouse fibroblasts disrupts assembly/stability of respiratory complexes I and IV. *J. Biol. Chem.* **284,** 4383–4391 (2009).
24. Li, K. *et al.* Cytochrome *c* deficiency causes embryonic lethality and attenuates stress-induced apoptosis. *Cell* **101,** 389–399 (2000).
25. Moon, S. H. *et al.* Activation of mitochondrial calcium-independent phospholipase A2g (iPLA2g) by divalent cations mediating arachidonate release and production of downstream eicosanoids. *J. Biol. Chem.* **287,** 14880–14895 (2012).
26. Krysko, D. V. *et al.* Emerging role of damage-associated molecular patterns derived from mitochondria in inflammation. *Trends Immunol.* **32,** 157–164 (2011).
27. Wilensky, R. L. *et al.* Inhibition of lipoprotein-associated phospholipase A2 reduces complex coronary atherosclerotic plaque development. *Nature Med.* **14,** 1059–1066 (2008).
28. Tyurin, V. A. *et al.* Specificity of lipoprotein-associated phospholipase A2 toward oxidized phosphatidylserines: liquid chromatography–electrospray ionization mass spectrometry characterization of products and computer modeling of interactions. *Biochemistry* **51,** 9736–9750 (2012).
29. David, S., Greenhalgh, A. D. & Lopez-Vales, R. Role of phospholipase A2s and lipid mediators in secondary damage after spinal cord injury. *Cell Tissue Res.* **349,** 249–267 (2012).
30. Dennis, E. A., Cao, J., Hsu, Y. H., Magrioti, V. & Kokotos, G. Phospholipase A2 enzymes: physical structure, biological function, disease implication, chemical inhibition, and therapeutic intervention. *Chem. Rev.* **111,** 6130–6185 (2011).
31. Daum, G., Lees, N. D., Bard, M. & Dickson, R. Biochemistry, cell biology and molecular biology of lipids of *Saccharomyces cerevisiae*. *Yeast* **14,** 1471–1510 (1998).
32. Kagan, V. E. *et al.* Cytochrome *c*/cardiolipin relations in mitochondria: a kiss of death. *Free Radic. Biol. Med.* **46,** 1439–1453 (2009).
33. Basova, L. V. *et al.* Cardiolipin switch in mitochondria: shutting off the reduction of cytochrome *c* and turning on the peroxidase activity. *Biochemistry* **46,** 3423–3434 (2007).
34. Belikova, N. A. *et al.* Peroxidase activity and structural transitions of cytochrome *c* bound to cardiolipin-containing membranes. *Biochemistry* **45,** 4998–5009 (2006).
35. Belikova, N. A. *et al.* Heterolytic reduction of fatty acid hydroperoxides by cytochrome *c*/cardiolipin complexes: antioxidant function in mitochondria. *J. Am. Chem. Soc.* **131,** 11288–11289 (2009).
36. Kim, I. C. Radioimmunoassay for testicular cytochrome *c* (ct). Evidence for the presence of apocytochrome ct pool in rat testis extract. *J. Biol. Chem.* **262,** 11156–11162 (1987).
37. Schug, Z. T. & Gottlieb, E. Cardiolipin acts as a mitochondrial signalling platform to launch apoptosis. *Biochim. Biophys. Acta* **1788,** 2022–2031 (2009).
38. Arnarez, C., Marrink, S. J. & Periole, X. Identification of cardiolipin binding sites on cytochrome *c* oxidase at the entrance of proton channels. *Sci. Rep.* **3,** 1263 (2013).
39. Liu, Z. *et al.* Remarkably high activities of testicular cytochrome *c* in destroying reactive oxygen species and in triggering apoptosis. *Proc. Natl Acad. Sci. USA* **103,** 8965–8970 (2006).
40. Kiebish, M. A. *et al.* Dysfunctional cardiac mitochondrial bioenergetic, lipidomic, and signaling in a murine model of Barth syndrome. *J. Lipid Res.* **54,** 1312–1325 (2013).
41. Davis, B. *et al.* Electrospray ionization mass spectrometry identifies substrates and products of lipoprotein-associated phospholipase A2 in oxidized human low density lipoprotein. *J. Biol. Chem.* **283,** 6428–6437 (2008).
42. Chu, C. T. *et al.* Cardiolipin externalization to the outer mitochondrial membrane acts as an elimination signal for mitophagy in neuronal cells. *Nature Cell Biol.* **15,** 1197–1205 (2013).
43. Garg, A. D. *et al.* Immunogenic cell death, DAMPs and anticancer therapeutics: an emerging amalgamation. *Biochim. Biophys. Acta* **1805,** 53–71 (2010).
44. Ray, N. B. *et al.* Dynamic regulation of cardiolipin by the lipid pump Atp8b1 determines the severity of lung injury in experimental pneumonia. *Nature Med.* **16,** 1120–1127 (2010).
45. Codina, R., Vanasse, A., Kelekar, A., Vezys, V. & Jemmerson, R. Cytochrome *c*-induced lymphocyte death from the outside in: inhibition by serum leucine-rich α-2-glycoprotein-1. *Apoptosis* **15,** 139–152 (2010).
46. Xu, L., Davis, T. A. & Porter, N. A. Rate constants for peroxidation of polyunsaturated fatty acids and sterols in solution and in liposomes. *J. Am. Chem. Soc.* **131,** 13037–13044 (2009).
47. Cheng, H. *et al.* Shotgun lipidomics reveals the temporally dependent, highly diversified cardiolipin profile in the mammalian brain: temporally coordinated postnatal diversification of cardiolipin molecular species with neuronal remodeling. *Biochemistry* **47,** 5869–5880 (2008).
48. Ji, J. *et al.* Lipidomics identifies cardiolipin oxidation as a mitochondrial target for redox therapy of brain injury. *Nature Neurosci.* **15,** 1407–1413 (2012).
49. Tyurina, Y. Y. *et al.* Oxidative lipidomics of gamma-radiation-induced lung injury: mass spectrometric characterization of cardiolipin and phosphatidylserine peroxidation. *Radiation Res.* **175,** 610–621 (2011).
50. Rouser, G., Fkeischer, S. & Yamamoto, A. Two dimensional then layer chromatographic separation of polar lipids and determination of phospholipids by phosphorus analysis of spots. *Lipids* **5,** 494–496 (1970).
51. Miller, T. M. *et al.* Rapid, simultaneous quantitation of mono and dioxygenated metabolites of arachidonic acid in human CSF and rat brain. *J. Chromatogr. B* **877,** 3991–4000 (2009).

Acknowledgements

We are thankful to J. L. Millan and S. Narisawa for providing the t-cyt *c*-specific antibody. We acknowledge support from the National Institutes of Health (ES020693, ES021068, U19AIO68021, PO1 HL114453, NS076511, NS061817, NS052315), the National Institute

for Occupational Safety and Health (OH008282), the National Center for Research Resources (S10RR023461), the Human Frontier Science Program (HFSP-RGP0013/2014) and the Fulbright US/Canada Scholar Program.

Author contributions

Y.Y.T. designed experiments, performed the MS analysis of CL and its oxidation and hydrolysis products *in vivo* and *in vitro* and co-wrote the manuscript, S.M.P. performed MS analysis of oxygenated species of arachidonic acid, V.A.T. performed experiments on CL hydrolysis by $LpPLA_2$ and MS analysis of CL and its hydrolysis products in the small intestine and cells, A.A.K. performed experiments on peroxidase activity of cyt *c*/CL complexes, J.J. performed the experiments on knocking down t-cyt *c*, T.S.A. and V.I.K. participated in the MS analysis of CL and its oxidation and hydrolysis products, A.S.V. and M-Y.J. performed cell and mitochondria experiments, D.M. and J.K.S. performed computational analysis of s-cyt *c* and t-cyt *c*, M.W.E. and J.S.G. contributed to the design and performance of the *in vivo* experiment (WBI), T.C.J. and P.M.K. participated in the design and performance of the *in vitro* experiments with neurons and astrocytes, Y.A.V. and B.R.P. participated in discussion of the results on LC/MS and aspects of the work with the hydrolysis of CL_{ox}, H.B. contributed to the formulation of the initial concept of the study, designed and participated in the performance of the *in vivo* experiment (CCI) and co-wrote the manuscript, and V.E.K. suggested the idea, designed the study and wrote the manuscript. All authors discussed the results and commented on the manuscript.

Additional information

Supplementary information is available in the online version of the paper. Reprints and permissions information is available online at www.nature.com/reprints. Correspondence and requests for materials should be addressed to Y.Y.T., H.B. and V.E.K.

Competing financial interests

The authors declare no competing financial interests.